Article

NADP-Dependent Malic Enzyme Genes in Sweet Pepper Fruits: Involvement in Ripening and Modulation by Nitric Oxide (NO)

Jorge Taboada [1], Salvador Gozález-Gordo [1], María Ángeles Muñoz-Vargas, José M Palma [*], FRANCISCO JAVIER CORPAS

Posted Date: 23 May 2023

doi: 10.20944/preprints202305.1587.v1

Keywords: cis-regulatory element; fruit ripening; malate; NADPH; NADP dehydrogenases; nitric oxide; pepper

Article

NADP-dependent Malic Enzyme Genes in Sweet Pepper Fruits: Involvement in Ripening and Modulation by Nitric Oxide (NO)

Jorge Taboada †, Salvador González-Gordo †, María A Muñoz-Vargas, José M Palma * and Francisco J Corpas

Department of Stress, Development and Signaling in Plants, Group of Antioxidants, Free Radicals and Nitric Oxide in Biotechnology, Food and Agriculture, Estación Experimental del Zaidín (Spanish National Research Council, CSIC), C/Profesor Albareda, 1, 18008 Granada, Spain.

* Correspondence: josemanuel.palma@eez.csic.es

† These authors equally contributed to this work.

Abstract: NADPH is an indispensable cofactor in a wide range of physiological processes which is generated by a family of NADPH-dehydrogenases, where the NADP-dependent malic enzyme (NADP-ME) is one member of these enzymes. Pepper (*Capsicum annuum* L.) fruit is a horticultural product worldwide consumed which has great nutritional and economic relevance. Besides the phenotypical changes that undergo pepper fruit during ripening, there are many associated modifications at transcriptomic, proteome ic, biochemical, and metabolic levels. Nitric oxide (NO) is a recognized signal molecule that can exert regulatory functions in diverse plant processes. To our knowledge, there is very scarce information about the number of genes encoding for NADP-ME in pepper plants and their expression during the ripening of sweet pepper fruit. Based on a data-mining approach on the pepper plant genome and fruit transcriptome (RNA-seq), five *NADP-ME* genes were identified, and four of them, namely *CaNADP-ME2* to *CaNADP-ME5*, were expressed in fruit. The time-course expression analysis of these genes during different fruit ripening stages including green immature (G), breaking point (BP), and red ripe (R) showed that they were differentially modulated. Thus, while *CaNADP-ME3* and *CaNADP-ME5* were upregulated, *CaNADP-ME*2 and *CaNADP-ME4* were downregulated. Exogenous NO treatment of fruit triggered the downregulation of *CaNADP-ME4*. Furthermore, the analysis of the cis-regulatory elements showed that *CaNADP-ME2* and *CaNADP-ME5* were positively regulated by the light-responsive element Box4 whereas *CaNADP-ME4* was by ABRE (ACGT-containing abscisic acid response element), which is involved in the abscisic acid (ABA) responsiveness. To get deeper knowledge on this enzyme system from fruits, we obtained the 50-75% ammonium-sulfate-enriched protein fraction containing CaNADP-ME enzyme activity, and this was assayed by non-denaturing polyacrylamide gel electrophoresis (PAGE). The results allowed identifying four isozymes designated CaNADP-ME I to CaNADP-ME IV. Taken together, the data provide new pieces of information on the CaNADP-ME system with the identification of five *CaNADP-ME* genes and how the four genes expressed in pepper fruits are modulated during ripening and by exogenous NO gas treatment.

Keywords: cis-regulatory element; fruit ripening; malate; NADPH; NADP dehydrogenases; nitric oxide; pepper

1. Introduction

NADPH (reduced nicotinamide adenine dinucleotide phosphate) is a central cofactor in a wide range of biosynthetic pathways that are essential in the metabolism of the plant cells such as the Calvin cycle, carotenoids, fatty acids or the aromatic amino acids (Phe, Tyr, Trp) as well as proline [1–3]. Furthermore, NADPH also sustains cellular detoxification and defense, for example, it is necessary to support the glutathione reductase activity as part of the ascorbate-glutathione cycle, or the generation of superoxide radical by the NADPH oxidase (NOX), also designated as respiratory burst oxidase homolog (Rboh) [4–6]. But also NADPH is necessary for the nitric oxide (NO) generation through the L-arginine-dependent NO synthase-like activity [7].

 doi:10.20944/preprints202305.1587.v1

The NADP-dependent malic enzyme (NADP-ME, EC 1.1.1.40) is one of the NADPH-generating dehydrogenases that catalyzes the reversible oxidative decarboxylation of L-malate using $NADP^+$ as a coenzyme, to generate pyruvate, CO_2 and NADPH, in the presence of a bivalent cation either Mg^{2+} or Mn^{2+}. NADP-ME plays a multirole in plants [8,9] including seed germination [10], development [11], and fruit physiology [12–16], but also in the mechanism of response against diverse environmental stresses [17] including salinity [18–20], water stress [21,22], mechanical wounding [23], arsenic [24–26], chromium [27], herbicides [28], low-temperature [29], and potassium deficiency [30,31].

Pepper (*Capsicum annuum* L.) is an important horticultural crop whose fruit is worldwide consumed. It is characterized to contain a significant quantity of vitamin C, provitamin A, and mineral such as calcium as well as other compounds with healthy properties [32]. Recently, it has been shown that during the ripening of pepper fruits, there is an noteworthy metabolism of reactive oxygen and nitrogen species (ROS and RNS, respectively), which has associated a physiological nitro-oxidative stress, where different ROS-generating and antioxidant systems are differentially modulated [33–40]. Previous studies have described that NADP-ME activity is modulated during the ripening of pepper fruit [41,42] but, to our knowledge, there is not any information about the modulation of genes that code for NADP-MEs in pepper fruits. Therefore, the main goal of this study was to identify the *NADP-ME* genes in pepper fruits and how they are modulated during ripening and by the effect of the exogenous application of NO. Additionally, four CaNADP-ME isoenzymatic activities were detected in fruits.

2. Results

2.1. Identification of the NADP-ME Genes in Pepper (Capsicum annuum L.): Sequence and Cis-Regulatory Elements

Based on the available NADP-ME sequences in *Arabidopsis thaliana*, the analysis of the *Capsicum annuum* L. genome has allowed us to identify five *NADP-ME* genes designated *CaNADP-ME1* to *CaNADP-ME5*, each one distributed in chromosomes (Chr) 3, 5, 8, 9, and 12, respectively. On the other hand, from data-mining of the transcriptome obtained in sweet pepper fruits [33], four of these genes, *CaNADP-ME2* to *CaNADP-ME5*, were identified, indicated in red color in**Table 1.** Some properties of these five genes and their corresponding encoded proteins including the number of amino acids (aa), molecular mass (kDa), and their putative subcellular localization were also recapitulated (Table 1).

Table 1. Summary of the five NADP-dependent malic enzyme (*NADP-ME*) genes identified in the pepper (*Capsicum annuum* L.) genome and some of the properties related to the protein encoded for these genes including the number of amino acids (aa), molecular mass (kDa), theoretical pI and their subcellular localization. The 4 *CaNADP-ME* genes specifically detected in the sweet pepper fruit transcriptome are highlighted in red.

Gene Name	Gene ID	Chr.	Genomic Location	Protein ID	Length (aa)	Da	Theoretical pI	Subcellular localization
CaNADP-ME1	107861795	3	267357814-267362949	XP_047266087.1	643	70,840	5.94	Plastid
CaNADP-ME2	107843507	5	158139423-158145651	XP_016543302.1	578	64,245	5.80	Cytosol
CaNADP-ME3	107847755	8	26364857-26372640	XP_016547705.1	618	68,468	6.57	Plastid
CaNADP-ME4	107842298	9	199489875-199498766	XP_016541547.1	590	65,360	6.13	Plastid
CaNADP-ME5	107850438	12	97276100-97283614	XP_016550447.1	644	70,709	6.28	Plastid

The analysis of the genomic organization indicated that *CaNADP-ME1*, *CaNADP-ME3*, and *CaNADP-ME5*, comprise 20 exons and 19 introns, whereas *CaNADP-ME2* and *CaNADP-ME4* have 19 exons and 18 introns. What is remarkable is that the length of the introns is very different (see for example *CaNADP-ME1* and *CaNADP-ME4*), what makes the length of the corresponding genes oscillate between 5000 and 9000 nucleotides (**Figure 1**).

Preprints (www.preprints.org) | NOT PEER-REVIEWED | Posted: 23 May 2023 doi:10.20944/preprints202305.1587.v1

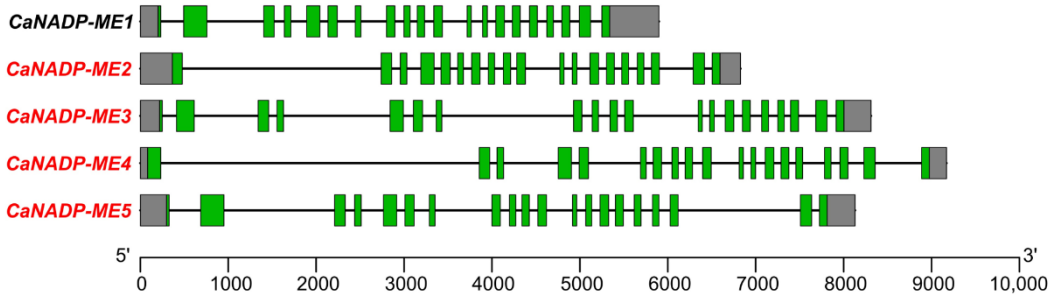

Figure 1. Genomic organization of the pepper *CaNADP-ME* gene family. The structure of the genes is shown with exons indicated by green boxes, and introns shown as black lines. Untranslated regions are shown by grey boxes. Exon–intron regions are drawn at scale.

As part of the characterization of these genes, the identification of cis-regulatory elements in 1500 upstream regions from the transcription starting point of the *CaNADP-ME* genes was accomplished. **Figure 2** displays the Heatmap analysis of 24 cis-regulatory elements of several families of elements involved in various processes including (i) light responsive; (ii) stress; and (iii) phytohormones. Nevertheless, ABRE (ACGT-containing abscisic acid response element) which is involved in the abscisic acid (ABA) responsiveness, was the cis-regulatory element that exert the most remarkable positive effect on *CaNADP-ME4*. This was followed by Box4, as part of the light-responsive family that affected positively *CaNADP-ME2* and *CaNADP-ME5*.

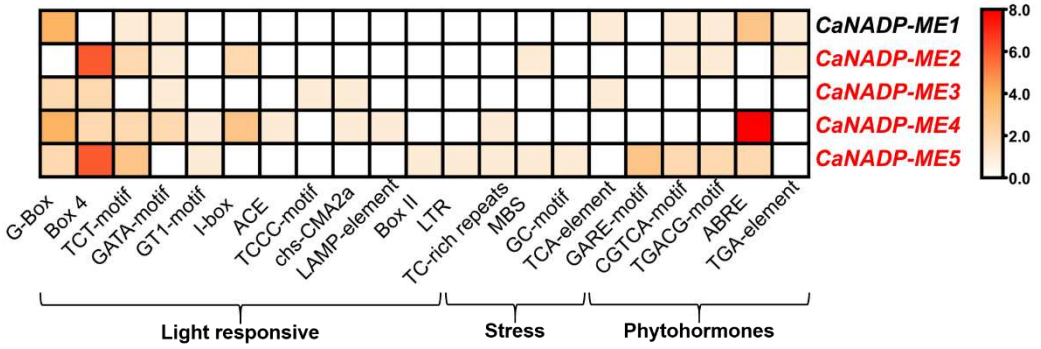

Figure 2. Heatmap of cis-regulatory elements corresponding to the 1500 bp upstream region from the transcription start point of *CaNADP-ME* genes. The cis-regulatory elements were grouped according to their functional implications including DNA, regulation and cell cycle, light responsive, stress and phytohormones. Motifs were identified in the PlantCARE database.

2.2. NADP-ME Proteins from Pepper: Sequence, Phylogenetic Analysis and Modeling

The protein analysis of the identified CaNADP-MEs (**Table 1**) indicates that the subunit molecular mass ranged from 64 kDa to 71 kDa, and they were distributed in the plastid and cytosol. The analysis of the primary structure of these CaNADP-MEs and their alignment allowed discriminating ten amino acid motifs. **Figure 3a** shows the distribution of these motifs in the different isozymes and **Figure 3b** illustrates the sequence of amino acids motifs where the height of each amino acid symbol is proportional to the degree of conservation in the consensus sequences. Based on previous information on the plant NADP-ME family [43–45], motif 1 contains the sequence VYTPTVGEAC which corresponds to the NADP-binding site 1. Nevertheless, a second putative NADP binding site recognized in maize NADP-ME corresponds to the sequence ILGLGDLGC, and it is also present in motif 2. On the other hand, motif 3 includes three residues involved in the metal binding which are E229, D330, and D354 (using the numbering of NADP-ME1). **Figure S1** shows the

Preprints (www.preprints.org) | NOT PEER-REVIEWED | Posted: 23 May 2023 doi:10.20944/preprints202305.1587.v1

amino acid alignment of these 5 CaNADP-MEs. The conserved residues involved in the binding of NADP and metal (Mg^{2+} or Mn^{2+}) are remarked with boxes.

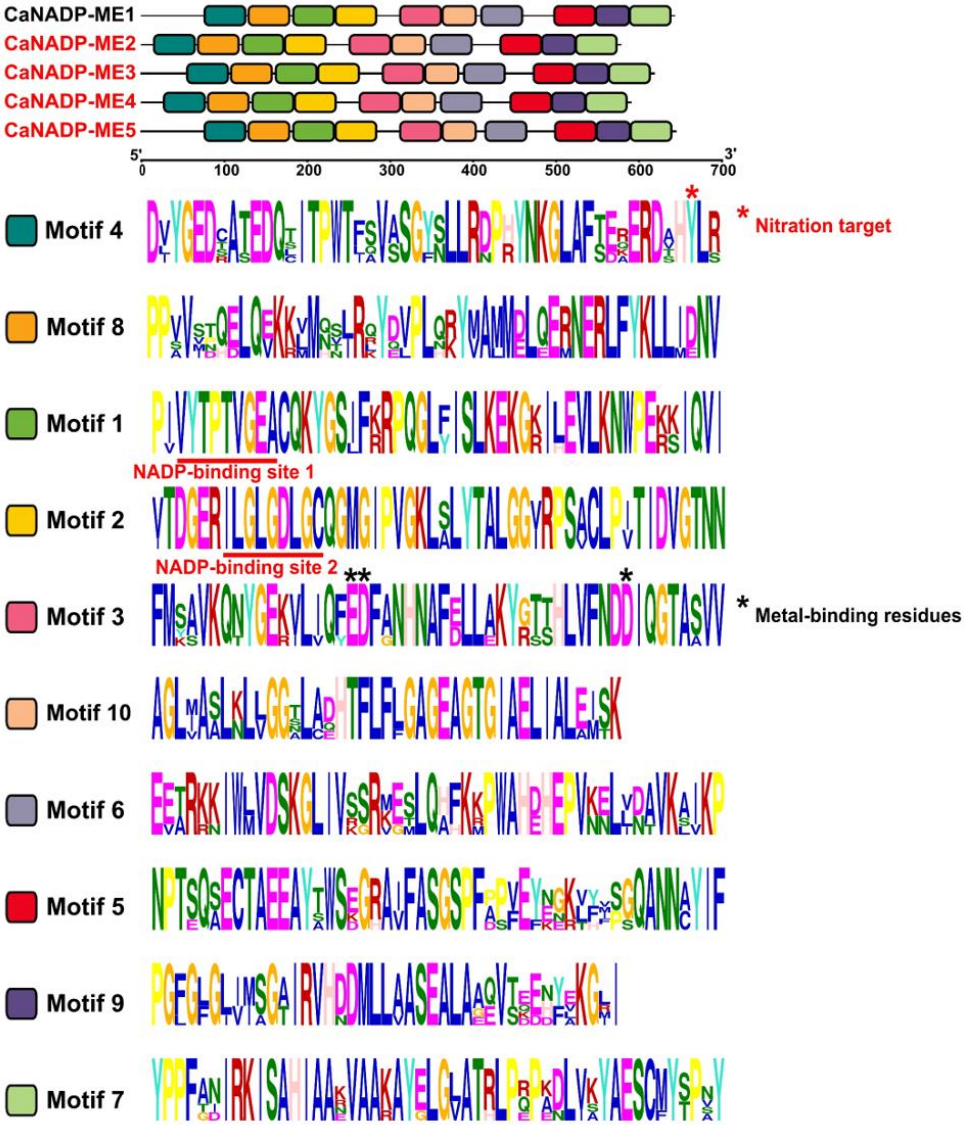

Figure 3. Identification and position of consensus amino acid motifs for pepper CaNADP-MEs. **(a)** Distribution of conserved motifs. The distribution of conserved motifs, numbers 1–10, are represented by boxes of different colors. **(b)** Amino acids sequence of the motifs. Ten amino acid motifs with various sizes were identified. The height of each amino acid symbol is proportional to the degree of conservation in the consensus sequences depicted in the ten motifs. Sequence logos of conserved motifs were created by MEME.

The phylogenetic analysis among the NADP-MEs from several plant species including pepper (*Capsicum annuum*), *Arabidopsis thaliana*, maize (*Zea mays*), grape (*Vitis vinifera*), bean (*Phaseolus vulgaris*), and rice (*Oryza sativa* subs. *japonica*), among others, allowed the finding of four main groups designated as I, II, III, and IV which are represented by different colors in **Figure 4**. The CaNADP-MEs found in pepper fruit are indicated in red. Group I, which includes CaNADP-ME2 and CaNADP-ME4, consists of both monocot and dicot plants. Groups III (CaNADP-ME1 and CaNADP-ME5) and IV (CaNADP-ME3) comprise dicot plants. On the other hand, group II is exclusive of monocots.

Preprints (www.preprints.org) | NOT PEER-REVIEWED | Posted: 23 May 2023 doi:10.20944/preprints202305.1587.v1

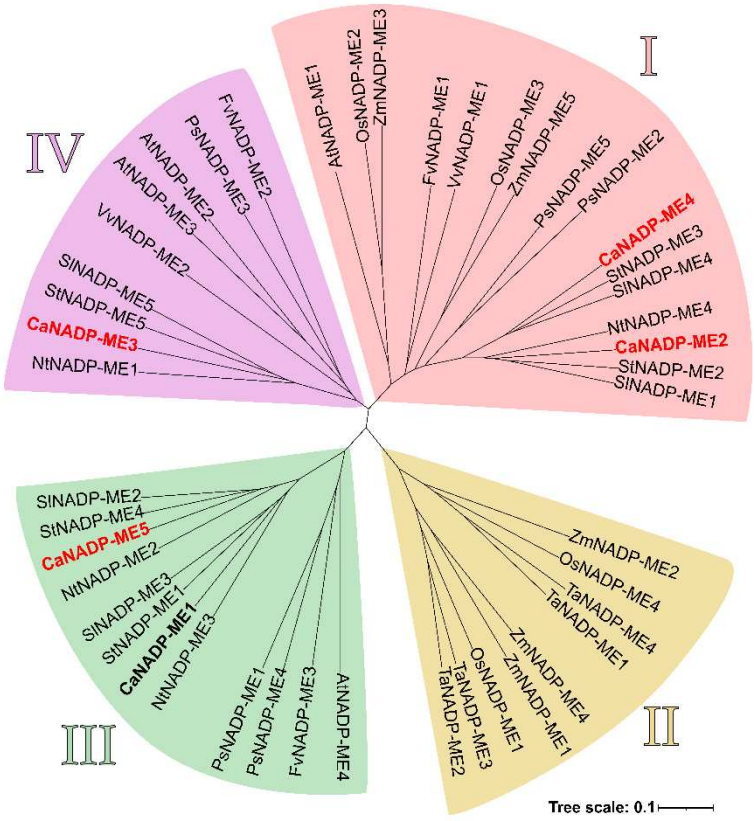

Figure 4. Phylogenetic relationships among NADP-MEs from different plant species. Clusters (I-IV) are displayed using different colors. The NADP-MEs identified in pepper are highlighted in bold. Those found specifically in the sweet pepper fruit are indicated in red. Species abbreviations: At (*Arabidopsis thaliana*), Ca (*Capsicum annuum*), Fv (*Fragaria vesca* subs. *vesca*), Nt (*Nicotiana tabacu*m), Os (*Oryza sativa* subs. *japonica*), Ps (*Pisum sativum*), Sl (*Solanum lycopersicum*), St (*Solanum tuberosum*), Ta (*Triticum aestivum*), Vv (*Vitis vinifera*), and Zm (*Zea mays*).

NADP-ME is considered to be a tetrameric enzyme [46], and **Figure 5** depicts the model of the quaternary structure of plastidial CaNADP-ME3 present in pepper fruits where it is remarked the binding sites for NADP and metals in each one of the subunits which are colored in yellow, green, cyan, and dark blue.

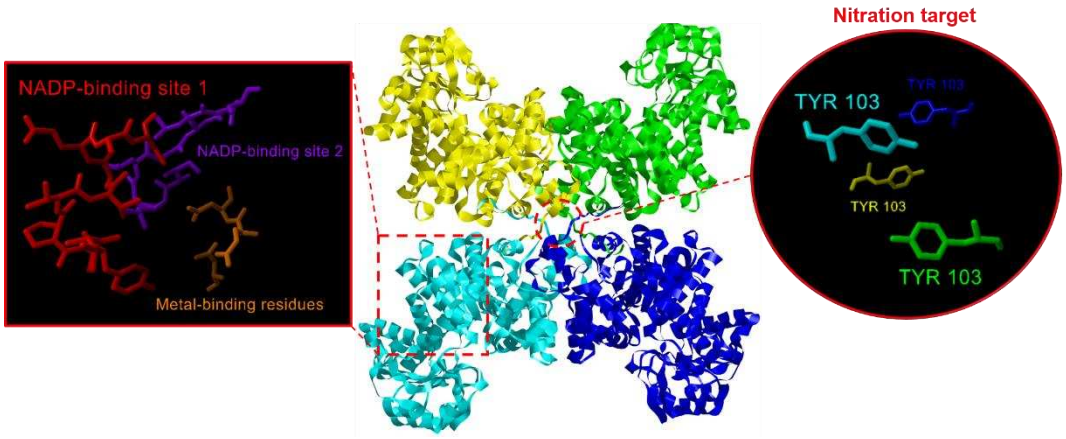

Figure 5. Model of the quaternary structure of CaNADP-ME3 present in pepper fruits. Subunits are colored in yellow, green, cyan, and dark blue. On the left, the amino acid residues involved in the binding of NADP and metals in one of the subunits are shown in detail. On the right, the binding site of the subunits is shown highlighting the Tyr107 residues which are considered as nitration targets.

Preprints (www.preprints.org) | NOT PEER-REVIEWED | Posted: 23 May 2023 doi:10.20944/preprints202305.1587.v1

2.3. Fruit CaNADP-ME Genes: Expression during Ripening and by Exogenous NO Treatment

The analysis of the RNAseq of sweet pepper fruits of the four CaNADP-ME genes was carried out at different ripening stages and after the exposition to exogenous NO gas. **Supplementary Figure S1** illustrates the experimental design which includes green immature (G), breaking point (BP1), and red ripe (R) fruits. Also, for the exposition to exogenous NO gas, two additional groups were established: fruits treated with 5 ppm NO for 1 h (BP2 + NO) and another group that was not treated with NO (BP2 − NO) corresponding to the control group. **Figure 6** shows the time-course analysis of the four genes identified in pepper fruits. CaNADP-ME3 and CaNADP-ME5 were upregulated during fruit ripening whereas CaNADP-ME2 and CaNADP-ME4 were downregulated. Exogenous NO treatment of fruit caused the downregulation of CaNADP-ME4 but the other genes were unaffected.

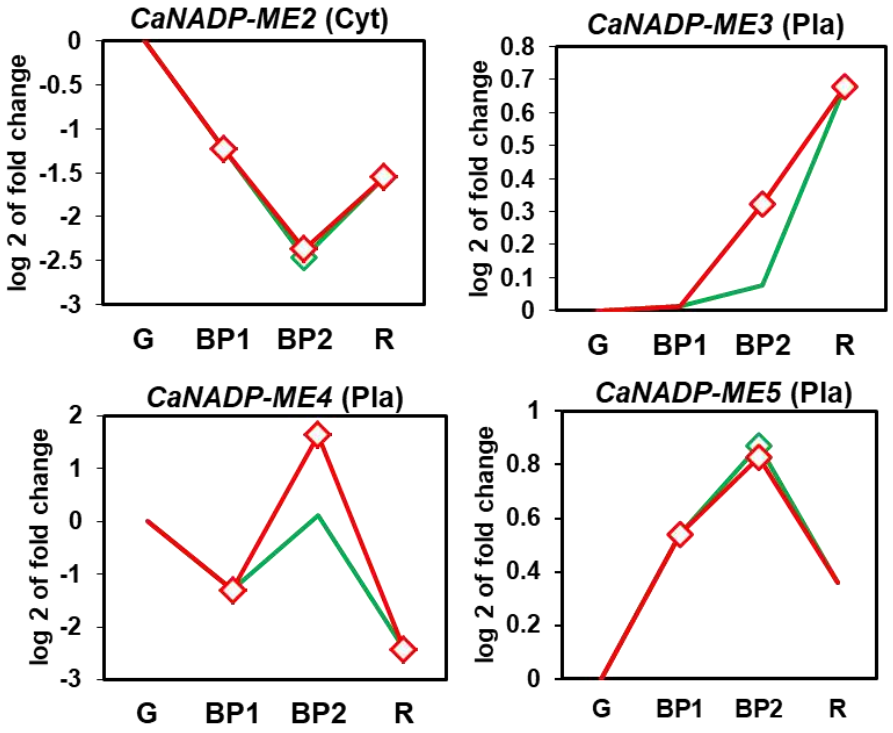

Figure 6. Time-course expression analysis of four *CaNADP-ME* genes (RNA-Seq) under natural ripening conditions and after exogenous NO treatment. Samples of sweet pepper fruits at different ripening stages correspond to immature green (G), breaking point 1 (BP1), breaking point 2 with (green line) and without (red line) NO treatment (BP2 + NO and BP2 – NO, respectively) and ripe red (R). Statistically significant changes in expression levels ($p < 0.05$) compared to green fruit (G) were indicated with diamonds.

2.4. Identification of the CaNADP-ME Isozymes in Pepper Fruits

To get deeper insights into the characterization of the CaNADP-ME enzyme system in pepper fruits, an in-gel analysis of the activity was accomplished. Due to previous assays showing the presence of very weak activity bands in crude extracts from pepper fruits, it was accomplished an enriched 50–75% ammonium-sulfate protein fractionation. **Figure 7** illustrates the enzymatic pattern of the CaNADP-ME isozymes detected in green pepper fruits. Using more than 240 µg protein of this enriched fraction, four isozymes were detected in polyacrylamide gels and were designated as CaNADP-ME I to CaNADP-ME IV, according to their increasing electrophoretic mobility. CaNADP-ME III and IV were the most abundant isozymes, representing 33 and 26%, respectively. This was followed by CaNADP-ME II (24%), and CaNADP-ME I (17%).

Preprints (www.preprints.org) | NOT PEER-REVIEWED | Posted: 23 May 2023 doi:10.20944/preprints202305.1587.v1

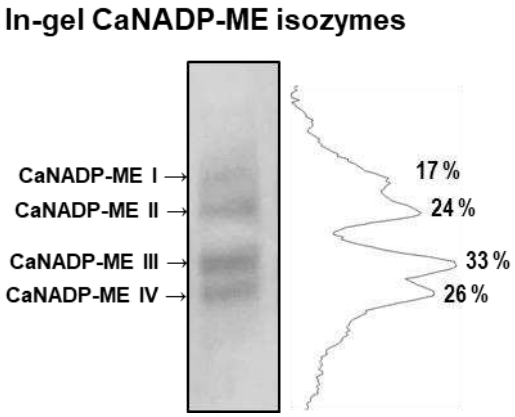

Figure 7. Isoenzymatic NADP-ME activity in green sweet pepper fruits in an enriched 50–75% ammonium-sulfate protein fraction. Protein samples (240 µg per lane) were separated by non-denaturing polyacrylamide gel electrophoresis (PAGE; 8% acrylamide), and activity was detected by the NBT method (left). NADP-ME isozymes were labeled I–IV. Densitometric analysis of these isozymes and their relative quantification (%) were made by the ImageJ program according to the isozyme profiles obtained (right).

3. Discussion

Higher plants contain several NADP-ME isozymes with different subcellular locations which play different functions. Usually, they are split into photosynthetic and non-photosynthetic isozymes according to their main physiological functions. Perhaps the best well-known function of chloroplast NADP-ME is the participation in the photosynthesis in the bundle sheath cells of C_4 plants which fix CO_2 into a molecule with four carbon atoms before starting the photosynthetic Calvin-Benson cycle [9,47,48], and also in Crassulacean acid metabolism (CAM) plants [49]. On the other hand, the designated non-photosynthetic NADP-MEs are present in the plastid and cytosol of all types of plants (C_3, C_4, and CAM). Other functions of the NADP-MEs are related to their involvement in malate equilibrium for stomatal movement [50] or pH regulation [51]. However, the generated NADPH is also needed for redox homeostasis [52,53] and in the mechanism of defense against diverse environmental stresses [1,29,54]. For example, in the response of Arabidopsis to the necrotrophic bacterium *Pectobacterium carotovorum*, it has been shown recently that NADP-ME2 is phosphorylated by the RPM1-INDUCED PROTEIN KINASE (RIPK) to increase the content of cytosolic NADPH, and this allows producing superoxide radical by the respiratory burst oxidase homolog D (RbohD) [6]

3.1. Pepper Genome Contains Five CaNADP-ME Genes but only Four Genes (CaNADP-ME2 to ME5) Are Expressed in Fruits

In previous studies, the presence of NADP-ME in pepper fruits was detected, where the activity increased during the fruit ripening. This suggested that this activity might cooperate with the supply of NADPH during this process [41,42], although it is also necessary for other enzymatic systems such as the Rboh whose activity increases [34], as well as for the lipid biosynthesis. However, to our knowledge, there is no information about the number of genes and isozymes of NADP-ME present in this non-climacteric fruit. The obtained data indicate that among the five *CaNADP-ME* genes detected in the pepper genome, only 4 were expressed in fruits that were differentially regulated during ripening and under an enriched NO atmosphere.

The number of exons/introns found in pepper *CaNADP-ME* genes is quite similar to those described for other higher plants. In the case of cytosolic *NADP-ME* from beans (*Phaseolus vulgaris* L.), the DNA sequencing of the unique gene allowed the identification of 20 exons [55]. In *Arabidopsis thaliana*, which contains four *NADP-ME* genes, it was found that *AtNADP-ME1* and *AtNADP-ME2* have 19 exons, but *AtNADP-ME3* and *AtNADP-ME4* have only 18 exons [56]. In maize (*Zea mays*), the *NADP-MEs* showed 19 encoding exons, except *cNADP-ME2* which has eight, because exons 12–

 doi:10.20944/preprints202305.1587.v1

19 are fused [45]. Intron sequences have multiple functions such as regulating alternative splicing, enhancing gene expression, control mRNA transport or chromatin assembly, among others [57,58]. However, in mammal genomes it has been suggested a alternation between the oldest exons, that is, the most conserved, and shorter introns. Conversely, longer introns tend to be between exons that are more contemporary [57]. In pepper, it is remarkable the observed difference in the intron length among the *CaNADP-ME* genes which can be until 4000 nucleotides. Considering the previous idea, it could be proposed that *CaNADP-ME1*, which contains the shortest introns, could have the oldest exons.

The encoding NADP-ME enzymes have a high degree of identity with other plant NADP-MEs and they have distinctive domains [45]. Furthermore, the predicted localization of the four identified CaNADP-MEs in fruits was one in the cytosol (CaNADP-ME2) and three in the plastids (CaNADP-ME5), what is analogous to other plant species [9,47,59,60]. Thus, in the model plant Arabidopsis, its genome contains four *NADP-ME* genes, and three encode for cytosolic isozymes (NADP-ME1 to NADP-ME3), whereas NADP-ME2 is located in plastids [61].

The available information on the NADP-ME in edible fruits is scarce. In the climacteric tomato fruits, the occurrence of NADP-ME has been associated with the relevance of malate in starch metabolism, thus affecting the fruit aging and postharvest softening [12,16,62]. In grape berries (*Vitis vinifera* L.) fruit, the NADP-ME contributes to the accumulation of malate during ripening [63]. In zucchini fruits, the storage at 15 °C for 2 days, followed by storage at 4 °C for 14 days, attenuates the chilling injury in the fruits, and the analysis of *NADP-ME* gene expression showed an increase which was accompanied by a concomitant enhancement of *G6PDH* (*glucose-6-phosphate dehydrogenase*) gene expression as well as an increase of the battery of antioxidant enzymes [64].

Metabolic analyses have shown that organic acids including malate and citrate are accumulated on a broad range of climacteric and non-climacteric fruits [65]. Thus, in some climacteric fruits malate is used as a substrate during the respiratory burst, whereas in non-climacteric malate is continually accumulated during ripening [66]. During hot pepper (*Capsicum chinense*) fruit development and ripening, malate content decreased during later developmental stages but it then increases during ripening [67]. Thus, it was suggested a correlation between malate levels and genes involved in the synthesis of starch [68]. A similar correlation was observed to genes associated with cell wall pathways and protein degradation [16]. Although these studies did not analyze the NADP-ME activity, however, it could be assumed that this activity should be involved in the total malate pool considering that the reaction catalyzed by this enzyme is reversible (L-malate ↔ pyruvate). Furthermore, these analyses could be puzzling if it is also considered the malate/oxaloacetate shuttles, a mechanism that involves several dicarboxylate translocators and malate dehydrogenase isozymes that catalyze the reversible interconversion of malate and oxaloacetate using either NAD or NADP, and are located in chloroplasts, mitochondria, and peroxisomes, thus allowing to modulate the ATP/NAD(P)H ratio [69]. Furthermore, malate metabolism also connects chloroplasts and mitochondrial ROS production [70]. All these organelles undergo drastic metabolic changes during pepper fruit ripening [71–73].

3.2. During Fruit Ripening, the Expression of the CaNADP-ME2 and ME4 are Downregulated whereas CaNADP-ME3 Are Upregulated. Exogenous NO Gas Exerts a Negative Modulation of CaNADP-ME3 and ME4

To our knowledge the available information about NO and NADP-ME at gene level is unknown. However, in a previous study, we found by in vitro assays that the NADP-ME activity of sweet pepper fruit was inhibited to a different degree in the presence of NO as well as by hydrogen sulfide (H_2S) donors [42]. This suggested that this enzyme could undergo posttranslational modifications mediated by these two molecules, including nitration, S-nitrosation, and persulfidation [74]. This was supported by proteomic studies in Arabidopsis where NADP-ME was identified to be a target of S-nitrosation [75] and persulfidation [76], although in any case the effect on the enzyme activity has been investigated.

 doi:10.20944/preprints202305.1587.v1

More recently, using a recombinant protein of the Arabidopsis cytosolic NADP-ME2 protein (NP_196728.1), mass spectrometry analyses corroborated that the Tyr73 could be nitrated and, consequently, it provoked the disruption of the interactions between the specific amino acids responsible for protein structure stability [29]. This equivalent Tyr residue is present in all the CaNADP-MEs and corresponds to the Tyr103 in the CaNADP-ME3; however, in a previous study, the preincubation of a 50–75% enriched $(NH_4)_2SO_4$ protein fraction, obtained from green pepper fruits containing the NADP-ME activity, with the nitrating peroxynitrite did not show any inhibitory effect [42], as it did in the Arabidopsis NADP-ME2. However, this apparent contradictory behavior can be explained by the fact that the enriched fruit fraction contains other NADP-MEs, and therefore each of them can be affected to a different degree. To corroborate it, it would be necessary to obtain the corresponding recombinant NADP-ME from pepper fruits and perform the corresponding assays, an issue which is being addressed in our laboratory.

4. Materials and Methods

4.1. Identification of the NADP-ME Genes in Pepper (Capsicum annuum L.), Chromosomal Location and Synteny Analysis

Different methodologies were used to ascertain the different NADP-ME-encoding genes in pepper. First, pepper proteome was downloaded from the NCBI database (Assembly UCD10Xv1.1; BioProject PRJNA814299; accessed on February 10, 2023). The amino acid sequences of NADP-MEs described in Arabidopsis thaliana were downloaded from the UnirProtKB database. These sequences were used as a query to search for NADP-MEs in the complete pepper proteome using the BLASTP tool. Second, the InterProScan tool was used [77] to confirm the presence of the conserved regions of the malic enzyme, an N-terminal domain (IPR012301) and the NAD(P) binding site (IPR012302).

Location coordinates of the identified CaNADP-MEs in the pepper genome were obtained from the NCBI database.

4.2. Phylogenetic and Conserved Motif Analyses of NADP-ME Protein Sequences

The identified NADP-ME protein sequences in pepper were used to construct a phylogenetic tree using the NADP-ME present in several plant sapecies (see Supplemental Table 1). The alignment of NADP-MEs was performed using the CLUSTALW method [78]. Then, the aligned sequences were subjected to MEGA11 [79] to perform an unrooted maximum likelihood phylogenetic tree with default parameters. Finally, the resulting phylogenetic tree was modified using the online tool Evolview v3 [80]. Conserved motifs of CaNADP-MEs were analyzed using the MEME tool [81] and visualized using TBtools software v1.108 [82]. The protein localization based on their amino acid sequences was predicted using several predictors: WoLF PSORT [83] and Plant-mSubP [84].

4.3. Introns/Exons and Cis-Regulatory Elements Analysis of the CaNADP-ME Genes

The distribution of introns and exons in the CaNADP-ME genes was obtained from the NCBI database. This information was drawn using the 'Basic Biosequence View' tool of the TBtools v1.108 software [82].

To predict putative promoter sequences of the identified CaNADP-ME genes obtained from the NCBI Nucleotide database (https://www.ncbi.nlm.nih.gov/nucleotide/; accessed on February 10, 2023), 1,500 bp upstream from the transcription starting point of each gene were considered. These sequences were searched for possible cis-acting regulatory elements using the PantCARE tool [85]. These results were manually processed and visualized using the 'Basic Biosequence View' function of TBtools v1.108 software [82].

4.4. Plant Material and Exogenous Nitric Oxide (NO) Gas Treatment

Sweet pepper (Capsicum annuum L. cultivar Melchor, California-type) fruits were collected from plants grown in commercial plastic-covered greenhouses (El Ejido, Almería, Spain). Fruits

without any external apparent injury were selected at three developmental stages: green immature (G), breaking point (BP1), and red ripe (R). The harvested fruits were placed in black plastic bags, transported to the laboratory at room temperature, washed with distilled water, and kept at a low temperature (about 7 °C ± 1 °C) for 24 h. To evaluate the effect of the exogenous NO gas treatment, we set two additional groups: fruits treated with 5 ppm NO for 1 h (BP2 + NO) and another group that was not treated with NO (BP2 − NO). After 3 days at room temperature, all fruits were chopped into small cubes (5 mm/edge), frozen under liquid nitrogen, and stored at -80 °C until use. **Supplementary Figure S2** shows the experimental design followed in this study with the representative phenotypes of sweet pepper fruits at the different ripening stages and subjected to NO treatment [33].

4.5. Library Preparation and RNA-Sequencing

All procedures were performed as previously described in [33] with minor modifications. Briefly, libraries were prepared using an Illumina protocol and were sequenced on an Illumina NextSeq550 platform using 2 × 75 bp paired-end reads. These reads were preprocessed to remove low-quality sequences. Useful reads were mapped against the set of transcripts available for Capsicum annuum species in the NCBI database (assembly UCD10Xv1.1; accessed on February 10, 2023) using Bowtie2 [86]. Transcript counts were obtained using Samtools [87].

Differential expression analyses were done using DEgenes-Hunter [88]. This R pipeline examined the relative change in expression between the different samples using different algorithms (EdgeR, DESeq2, Limma, and NOISeq) which apply their own normalizations and statistical tests to validate the whole experiment. On the other hand, an analysis of the time course of CaPODs gene expression was performed considering as reference the expression levels found in green fruits (G). Raw data are accessible at the Sequence Read Archive (SRA) repository under the accession PRJNA668052. This reference pepper fruit transcriptome and differentially expressed (DE) genes among the analyzed ripening stages and the NO treatment involved the analysis of 24 biological replicates corresponding to 5 replicates of each stage, except for green fruits that involved 4 replicates.

4.6. Fruit Extracts, Protein Assay, Protein Enrichment by Ammonium-Sulfate [$(NH_4)_2SO_4$] Fractionation and In-Gel Isozyme Profile of NADP-ME Activity

To obtain the crude extracts, fresh and intact green pepper fruits were used. The pericarps of the fruits were manually cut into longitudinal strips, and then into small pieces of approximately 0.5 cm^3. The pericarp sample was homogenized with a mortar and pestle in the presence of the extraction buffer in proportions 1:1 (w/v). Extraction buffer contained 50 mM Tris-HCl, 0.1 mM EDTA, 1 mM $MgCl_2$, 0.1% (v/v) Triton X-100, and 10% (v/v) glycerol. After homogenization, the extracts were filtered through two layers of nylon and centrifuged at 30,000 g for 20 min at 4°C. Protein concentration was determined using the Bio-Rad protein assay (Hercules, CA), with bovine serum albumin as standard.

Protein enrichment by ammonium-sulfate was done as previously described in [42]. Briefly, solid $(NH_4)_2SO_4$ was slowly added to the 30,000 *g* supernatant for 30 min of green pepper crude extracts up to a saturation of 50% (w/w). The solution was kept at 4 °C for about 30 min and then re-centrifuged at 30,000×g for 30 min, and the supernatant obtained was 75% (w/w) saturated by the slow addition of solid $(NH_4)_2SO_4$. The mix was centrifuged again, and the protein-enriched pellet obtained (50–75% fraction) was re-suspended in 0.1 M Tris-HCl buffer, pH 8.0, 1 mM EDTA, 0.1% (v/v) Triton X-100, 10% (v/v) glycerol. For 12 ml of original pepper extract the corresponding pellet was suspended in 1 ml. The enriched 50–75% protein fraction was loaded on a PD-10 desalting column containing Sephadex™ G-25 which enables high molecular weight substances (Mr > 5000) to be separated from

Non-denaturing PAGE was carried out in 6% acrylamide gels (19:1, acrylamide:bis-acrylamide ratio) using a Mini-Protean Tetra Cell (Bio-Rad, Hercules, CA, USA). Pepper fruit crude extracts were added 0.006% (w/v) bromophenol blue dye and then loaded onto gels. The NADP-ME isozymes were visualized by incubating the gels in a solution consisting of 50 mM Tris-HCl, pH 7.6, 0.8 mM NADP,

5 mM EDTA, 2 mM $MgCl_2$, 0.24 mM nitroblue tetrazolium, and 65 mM phenazine methosulfate containing 10 mM malate. When blue formazan bands appeared, the reaction was stopped by immersing the gels in 7% (v/v) acetic acid.

5. Conclusions

In a previous study on sweet pepper fruits, we studied the presence of NADP-ME activity as well as its regulation during ripening and in the presence of certain modulating molecules [41,42]. However, to our knowledge, there is no information on the number of genes that code for the pepper NADP-ME isozymes, which of them are expressed in fruits, and how they are modulated during ripening. Accordingly, the present data responds to these questions. Thus, pepper fruits express 4 *CaNADP-ME* genes that are differentially regulated during ripening and in the presence of exogenous NO. Likewise, four NADP-ME isoenzymes were identified in green fruits (NADP-ME I to NADP-ME4), where NADP-ME III and IV are the most prominent. However, future studies are necessary to unravel the role of each NADP-ME isoenzyme during fruit ripening, considering that both malate and the reducing power generated during their reaction in the form of NADPH are involved in numerous metabolic processes that undergo continuous adaptive changes during the fruit ripening.

Supplementary Materials: The following supporting information can be downloaded at the website of this paper posted on Preprints.org. **Supplementary Figure S1**: Alignment of the five CaNADP-ME sequences identifying the conserved NADP (blue) and metal binding (green) sites and the possible tyrosine (Tyr) residue capable of being nitrated (orange). Asterisks denote the conserved aminoacids. **Supplementary Figure S2**: Illustrative picture showing the experimental design used in this study with the representative phenotype of sweet pepper (*Capsicum annuum* L.) fruits at different stages and treatments: immature green, breaking point 1 (BP1), breaking point 2 without NO treatment (BP2 – NO), breaking point 2 with NO treatment (BP2 + NO), and ripe red. Fruits were subjected to a NO-enriched atmosphere (5 ppm) in a hermetic box for 1 h and were then stored at room temperature (RT) for 3 days. Reproduced with permission from González-Gordo et al. (2022).

Author Contributions: J.T., S.G.-G., and M.A.M.-V. performed biochemical and bioinformatics analyses. F.J.C. and J.M.P. designed the work, drove and coordinated the tasks. F.J.C. and J.M.P. wrote the first draft of the manuscript. All authors have read and agreed to the published version of the manuscript.

Funding: Our research is supported by a European Regional Development Fund co-financed grants from the Ministry of Science and Innovation (PID2019-103924GB-I00 and CPP2021-008703) and Junta de Andalucía (P18-274 FR-1359), Spain.

Data Availability Statement: Sequence Read Archive (SRA) data are available at the following link https://www.ncbi.nlm.nih.gov/sra/PRJNA668052 (accessed on 28 May 2020).

Acknowledgments: The provision of pepper fruits by Syngenta Seeds Ltd. (El Ejido, Almería, Spain) is acknowledged, especially Víctor J. Domínguez, Lidia Martín, and Manuel Solís. The valuable technical assistance of Mr. Carmelo Ruiz-Torres and Mrs. María J. Campos is deeply acknowledged.

Conflicts of Interest: The authors declare no conflict of interest.

References

1. Corpas, F.J.; Barroso, J.B. NADPH-Generating Dehydrogenases: Their Role in the Mechanism of Protection against Nitro-Oxidative Stress Induced by Adverse Environmental Conditions. *Frontiers in Environmental Science* **2014**, *2*.
2. Habashi, R.; Hacham, Y.; Dhakarey, R.; Matityahu, I.; Holland, D.; Tian, L.; Amir, R. Elucidating the Role of Shikimate Dehydrogenase in Controlling the Production of Anthocyanins and Hydrolysable Tannins in the Outer Peels of Pomegranate. *BMC Plant Biol* **2019**, *19*, 476. https://doi.org/10.1186/s12870-019-2042-1.
3. Meeks, K.R.; Tanner, J.J. Expression and Kinetic Characterization of PYCR3. *Arch Biochem Biophys* **2023**, *733*, 109468. https://doi.org/10.1016/j.abb.2022.109468.
4. Sagi, M.; Fluhr, R. Production of Reactive Oxygen Species by Plant NADPH Oxidases. *Plant Physiol* **2006**, *141*, 336–340. https://doi.org/10.1104/pp.106.078089.
5. Kaya, H.; Takeda, S.; Kobayashi, M.J.; Kimura, S.; Iizuka, A.; Imai, A.; Hishinuma, H.; Kawarazaki, T.; Mori, K.; Yamamoto, Y.; et al. Comparative Analysis of the Reactive Oxygen Species-Producing Enzymatic Activity of Arabidopsis NADPH Oxidases. *Plant J* **2019**, *98*, 291–300. https://doi.org/10.1111/tpj.14212.

6. Wu, B.; Li, P.; Hong, X.; Xu, C.; Wang, R.; Liang, Y. The Receptor-like Cytosolic Kinase RIPK Activates NADP-Malic Enzyme 2 to Generate NADPH for Fueling ROS Production. *Mol Plant* **2022**, *15*, 887–903. https://doi.org/10.1016/j.molp.2022.03.003.
7. Corpas, F.J.; González-Gordo, S.; Palma, J.M. NO Source in Higher Plants: Present and Future of an Unresolved Question. *Trends Plant Sci* **2022**, *27*, 116–119. https://doi.org/10.1016/j.tplants.2021.11.016.
8. Edwards, G.E.; Andreo, C.S. NADP-Malic Enzyme from Plants. *Phytochemistry* **1992**, *31*, 1845–1857. https://doi.org/10.1016/0031-9422(92)80322-6.
9. Drincovich, M.F.; Casati, P.; Andreo, C.S. NADP-Malic Enzyme from Plants: A Ubiquitous Enzyme Involved in Different Metabolic Pathways. *FEBS Lett* **2001**, *490*, 1–6. https://doi.org/10.1016/s0014-5793(00)02331-0.
10. Yazdanpanah, F.; Maurino, V.G.; Mettler-Altmann, T.; Buijs, G.; Bailly, M.N.; Karimi Jashni, M.; Willems, L.; Sergeeva, L.I.; Rajjou, L.C.; Hilhorst, H.W.M.; et al. NADP-MALIC ENZYME 1 Affects Germination after Seed Storage in Arabidopsis Thaliana. *Plant Cell Physiol* **2019**, *60*, 318–328. https://doi.org/10.1093/pcp/pcy213.
11. Airaki, M.; Leterrier, M.; Valderrama, R.; Chaki, M.; Begara-Morales, J.C.; Barroso, J.B.; del Río, L.A.; Palma, J.M.; Corpas, F.J. Spatial and Temporal Regulation of the Metabolism of Reactive Oxygen and Nitrogen Species during the Early Development of Pepper (Capsicum Annuum) Seedlings. *Ann Bot* **2015**, *116*, 679–693. https://doi.org/10.1093/aob/mcv023.
12. Goodenough, P.W.; Prosser, I.M.; Young, K. NADP-Linked Malic Enzyme and Malate Metabolism in Ageing Tomato Fruit. *Phytochemistry* **1985**, *24*, 1157–1162. https://doi.org/10.1016/S0031-9422(00)81093-6.
13. Franke, K.E.; Adams, D.O. Cloning of a Full-Length CDNA for Malic Enzyme (EC 1.1.1.40) from Grape Berries. *Plant Physiol* **1995**, *107*, 1009–1010. https://doi.org/10.1104/pp.107.3.1009.
14. Famiani, F.; Walker, R.P.; Técsi, L.; Chen, Z.H.; Proietti, P.; Leegood, R.C. An Immunohistochemical Study of the Compartmentation of Metabolism during the Development of Grape (Vitis Vinifera L.) Berries. *J Exp Bot* **2000**, *51*, 675–683.
15. Famiani, F.; Casulli, V.; Baldicchi, A.; Battistelli, A.; Moscatello, S.; Walker, R.P. Development and Metabolism of the Fruit and Seed of the Japanese Plum Ozark Premier (Rosaceae). *J Plant Physiol* **2012**, *169*, 551–560. https://doi.org/10.1016/j.jplph.2011.11.020.
16. Osorio, S.; Vallarino, J.G.; Szecowka, M.; Ufaz, S.; Tzin, V.; Angelovici, R.; Galili, G.; Fernie, A.R. Alteration of the Interconversion of Pyruvate and Malate in the Plastid or Cytosol of Ripening Tomato Fruit Invokes Diverse Consequences on Sugar but Similar Effects on Cellular Organic Acid, Metabolism, and Transitory Starch Accumulation. *Plant Physiol* **2013**, *161*, 628–643. https://doi.org/10.1104/pp.112.211094.
17. Chen, Q.; Wang, B.; Ding, H.; Zhang, J.; Li, S. Review: The Role of NADP-Malic Enzyme in Plants under Stress. *Plant Sci* **2019**, *281*, 206–212. https://doi.org/10.1016/j.plantsci.2019.01.010.
18. Valderrama, R.; Corpas, F.J.; Carreras, A.; Gómez-Rodríguez, M.V.; Chaki, M.; Pedrajas, J.R.; Fernández-Ocaña, A.; Del Río, L.A.; Barroso, J.B. The Dehydrogenase-Mediated Recycling of NADPH Is a Key Antioxidant System against Salt-Induced Oxidative Stress in Olive Plants. *Plant Cell Environ* **2006**, *29*, 1449–1459. https://doi.org/10.1111/j.1365-3040.2006.01530.x.
19. Manai, J.; Gouia, H.; Corpas, F.J. Redox and Nitric Oxide Homeostasis Are Affected in Tomato (Solanum Lycopersicum) Roots under Salinity-Induced Oxidative Stress. *J. Plant Physiol.* **2014**, *171*, 1028–1035. https://doi.org/10.1016/j.jplph.2014.03.012.
20. Bouthour, D.; Kalai, T.; Chaffei, H.C.; Gouia, H.; Corpas, F.J. Differential Response of NADP-Dehydrogenases and Carbon Metabolism in Leaves and Roots of Two Durum Wheat (Triticum Durum Desf.) Cultivars (Karim and Azizi) with Different Sensitivities to Salt Stress. *J. Plant Physiol.* **2015**, *179*, 56–63. https://doi.org/10.1016/j.jplph.2015.02.009.
21. Signorelli, S.; Corpas, F.J.; Borsani, O.; Barroso, J.B.; Monza, J. Water Stress Induces a Differential and Spatially Distributed Nitro-Oxidative Stress Response in Roots and Leaves of Lotus Japonicus. *Plant Sci.* **2013**, *201–202*, 137–146. https://doi.org/10.1016/j.plantsci.2012.12.004.
22. Doubnerová Hýsková, V.; Miedzińska, L.; Dobrá, J.; Vankova, R.; Ryšlavá, H. Phosphoenolpyruvate Carboxylase, NADP-Malic Enzyme, and Pyruvate, Phosphate Dikinase Are Involved in the Acclimation of Nicotiana Tabacum L. to Drought Stress. *J Plant Physiol* **2014**, *171*, 19–25. https://doi.org/10.1016/j.jplph.2013.10.017.
23. Houmani, H.; Rodríguez-Ruiz, M.; Palma, J.M.; Corpas, F.J. Mechanical Wounding Promotes Local and Long Distance Response in the Halophyte Cakile Maritima through the Involvement of the ROS and RNS Metabolism. *Nitric Oxide* **2018**, *74*, 93–101. https://doi.org/10.1016/j.niox.2017.06.008.
24. Corpas, F.J.; Aguayo-Trinidad, S.; Ogawa, T.; Yoshimura, K.; Shigeoka, S. Activation of NADPH-Recycling Systems in Leaves and Roots of Arabidopsis Thaliana under Arsenic-Induced Stress Conditions Is Accelerated by Knock-out of Nudix Hydrolase 19 (AtNUDX19) Gene. *J Plant Physiol* **2016**, *192*, 81–89. https://doi.org/10.1016/j.jplph.2016.01.010.
25. Ruíz-Torres, C.; Feriche-Linares, R.; Rodríguez-Ruíz, M.; Palma, J.M.; Corpas, F.J. Arsenic-Induced Stress Activates Sulfur Metabolism in Different Organs of Garlic (Allium Sativum L.) Plants Accompanied by a

General Decline of the NADPH-Generating Systems in Roots. *J Plant Physiol* **2017**, *211*, 27–35. https://doi.org/10.1016/j.jplph.2016.12.010.

26. Rodríguez-Ruiz, M.; Aparicio-Chacón, M.V.; Palma, J.M.; Corpas, F.J. Arsenate Disrupts Ion Balance, Sulfur and Nitric Oxide Metabolisms in Roots and Leaves of Pea (Pisum Sativum L.) Plants. *Environmental and Experimental Botany* **2019**, *161*, 143–156. https://doi.org/10.1016/j.envexpbot.2018.06.028.
27. Kharbech, O.; Houmani, H.; Chaoui, A.; Corpas, F.J. Alleviation of Cr(VI)-Induced Oxidative Stress in Maize (Zea Mays L.) Seedlings by NO and H2S Donors through Differential Organ-Dependent Regulation of ROS and NADPH-Recycling Metabolisms. *J. Plant Physiol.* **2017**, *219*, 71–80. https://doi.org/10.1016/j.jplph.2017.09.010.
28. de Freitas-Silva, L.; Rodríguez-Ruiz, M.; Houmani, H.; da Silva, L.C.; Palma, J.M.; Corpas, F.J. Glyphosate-Induced Oxidative Stress in Arabidopsis Thaliana Affecting Peroxisomal Metabolism and Triggers Activity in the Oxidative Phase of the Pentose Phosphate Pathway (OxPPP) Involved in NADPH Generation. *J Plant Physiol* **2017**, *218*, 196–205. https://doi.org/10.1016/j.jplph.2017.08.007.
29. Begara-Morales, J.C.; Sánchez-Calvo, B.; Gómez-Rodríguez, M.V.; Chaki, M.; Valderrama, R.; Mata-Pérez, C.; López-Jaramillo, J.; Corpas, F.J.; Barroso, J.B. Short-Term Low Temperature Induces Nitro-Oxidative Stress That Deregulates the NADP-Malic Enzyme Function by Tyrosine Nitration in Arabidopsis Thaliana. *Antioxidants (Basel)* **2019**, *8*, 448. https://doi.org/10.3390/antiox8100448.
30. Sánchez-McSweeney, A.; González-Gordo, S.; Aranda-Sicilia, M.N.; Rodríguez-Rosales, M.P.; Venema, K.; Palma, J.M.; Corpas, F.J. Loss of Function of the Chloroplast Membrane K+/H+ Antiporters AtKEA1 and AtKEA2 Alters the ROS and NO Metabolism but Promotes Drought Stress Resilience. *Plant Physiol Biochem* **2021**, *160*, 106–119. https://doi.org/10.1016/j.plaphy.2021.01.010.
31. Houmani, H.; Debez, A.; Freitas-Silva, L. de; Abdelly, C.; Palma, J.M.; Corpas, F.J. Potassium (K+) Starvation-Induced Oxidative Stress Triggers a General Boost of Antioxidant and NADPH-Generating Systems in the Halophyte Cakile Maritima. *Antioxidants (Basel)* **2022**, *11*, 401. https://doi.org/10.3390/antiox11020401.
32. Guevara, L.; Domínguez-Anaya, M.Á.; Ortigosa, A.; González-Gordo, S.; Díaz, C.; Vicente, F.; Corpas, F.J.; Pérez Del Palacio, J.; Palma, J.M. Identification of Compounds with Potential Therapeutic Uses from Sweet Pepper (Capsicum Annuum L.) Fruits and Their Modulation by Nitric Oxide (NO). *Int J Mol Sci* **2021**, *22*, 4476. https://doi.org/10.3390/ijms22094476.
33. González-Gordo, S.; Bautista, R.; Claros, M.G.; Cañas, A.; Palma, J.M.; Corpas, F.J. Nitric Oxide-Dependent Regulation of Sweet Pepper Fruit Ripening. *J Exp Bot* **2019**, *70*, 4557–4570. https://doi.org/10.1093/jxb/erz136.
34. González-Gordo, S.; Rodríguez-Ruiz, M.; Palma, J.M.; Corpas, F.J. Superoxide Radical Metabolism in Sweet Pepper (Capsicum Annuum L.) Fruits Is Regulated by Ripening and by a NO-Enriched Environment. *Front Plant Sci* **2020**, *11*, 485. https://doi.org/10.3389/fpls.2020.00485.
35. González-Gordo, S.; Rodríguez-Ruiz, M.; López-Jaramillo, J.; Muñoz-Vargas, M.A.; Palma, J.M.; Corpas, F.J. Nitric Oxide (NO) Differentially Modulates the Ascorbate Peroxidase (APX) Isozymes of Sweet Pepper (Capsicum Annuum L.) Fruits. *Antioxidants (Basel)* **2022**, *11*, 765. https://doi.org/10.3390/antiox11040765.
36. González-Gordo, S.; Cañas, A.; Muñoz-Vargas, M.A.; Palma, J.M.; Corpas, F.J. Lipoxygenase (LOX) in Sweet and Hot Pepper (Capsicum Annuum L.) Fruits during Ripening and under an Enriched Nitric Oxide (NO) Gas Atmosphere. *Int J Mol Sci* **2022**, *23*, 15211. https://doi.org/10.3390/ijms232315211.
37. González-Gordo, S.; Palma, J.M.; Corpas, F.J. Small Heat Shock Protein (SHSP) Gene Family from Sweet Pepper (Capsicum Annuum L.) Fruits: Involvement in Ripening and Modulation by Nitric Oxide (NO). *Plants (Basel)* **2023**, *12*, 389. https://doi.org/10.3390/plants12020389.
38. Palma, J.M.; Terán, F.; Contreras-Ruiz, A.; Rodríguez-Ruiz, M.; Corpas, F.J. Antioxidant Profile of Pepper (Capsicum Annuum L.) Fruits Containing Diverse Levels of Capsaicinoids. *Antioxidants (Basel)* **2020**, *9*, 878. https://doi.org/10.3390/antiox9090878.
39. Rodríguez-Ruiz, M.; Mioto, P.; Palma, J.M.; Corpas, F.J. S-Nitrosoglutathione Reductase (GSNOR) Activity Is down-Regulated during Pepper (Capsicum Annuum L.) Fruit Ripening. *Nitric Oxide* **2017**, *68*, 51–55. https://doi.org/10.1016/j.niox.2016.12.011.
40. Rodríguez-Ruiz, M.; González-Gordo, S.; Cañas, A.; Campos, M.J.; Paradela, A.; Corpas, F.J.; Palma, J.M. Sweet Pepper (Capsicum Annuum L.) Fruits Contain an Atypical Peroxisomal Catalase That Is Modulated by Reactive Oxygen and Nitrogen Species. *Antioxidants (Basel)* **2019**, *8*, 374. https://doi.org/10.3390/antiox8090374.
41. Mateos, R.M.; Bonilla-Valverde, D.; del Río, L.A.; Palma, J.M.; Corpas, F.J. NADP-Dehydrogenases from Pepper Fruits: Effect of Maturation. *Physiol Plant* **2009**, *135*, 130–139. https://doi.org/10.1111/j.1399-3054.2008.01179.x.
42. Muñoz-Vargas, M.A.; González-Gordo, S.; Palma, J.M.; Corpas, F.J. Inhibition of NADP-Malic Enzyme Activity by H2 S and NO in Sweet Pepper (Capsicum Annuum L.) Fruits. *Physiol Plant* **2020**, *168*, 278–288. https://doi.org/10.1111/ppl.13000.
43. Rothermel, B.A.; Nelson, T. Primary Structure of the Maize NADP-Dependent Malic Enzyme. *J Biol Chem* **1989**, *264*, 19587–19592.

44. Börsch, D.; Westhoff, P. Primary Structure of NADP-Dependent Malic Enzyme in the Dicotyledonous C4 Plant Flaveria Trinervia. *FEBS Lett* **1990**, *273*, 111–115. https://doi.org/10.1016/0014-5793(90)81063-t.
45. Tronconi, M.A.; Andreo, C.S.; Drincovich, M.F. Chimeric Structure of Plant Malic Enzyme Family: Different Evolutionary Scenarios for NAD- and NADP-Dependent Isoforms. *Front Plant Sci* **2018**, *9*, 565. https://doi.org/10.3389/fpls.2018.00565.
46. Detarsio, E.; Alvarez, C.E.; Saigo, M.; Andreo, C.S.; Drincovich, M.F. Identification of Domains Involved in Tetramerization and Malate Inhibition of Maize C4-NADP-Malic Enzyme. *J Biol Chem* **2007**, *282*, 6053–6060. https://doi.org/10.1074/jbc.M609436200.
47. Saigo, M.; Alvarez, C.E.; Andreo, C.S.; Drincovich, M.F. Plastidial NADP-Malic Enzymes from Grasses: Unraveling the Way to the C4 Specific Isoforms. *Plant Physiol Biochem* **2013**, *63*, 39–48. https://doi.org/10.1016/j.plaphy.2012.11.009.
48. Zhao, H.; Wang, Y.; Lyu, M.-J.A.; Zhu, X.-G. Two Major Metabolic Factors for an Efficient NADP-Malic Enzyme Type C4 Photosynthesis. *Plant Physiol* **2022**, *189*, 84–98. https://doi.org/10.1093/plphys/kiac051.
49. Honda, H.; Akagi, H.; Shimada, H. An Isozyme of the NADP-Malic Enzyme of a CAM Plant, Aloe Arborescens, with Variation on Conservative Amino Acid Residues. *Gene* **2000**, *243*, 85–92. https://doi.org/10.1016/s0378-1119(99)00556-9.
50. Laporte, M.M.; Shen, B.; Tarczynski, M.C. Engineering for Drought Avoidance: Expression of Maize NADP-Malic Enzyme in Tobacco Results in Altered Stomatal Function. *J Exp Bot* **2002**, *53*, 699–705. https://doi.org/10.1093/jexbot/53.369.699.
51. Arias, C.L.; Andreo, C.S.; Drincovich, M.F.; Gerrard Wheeler, M.C. Fumarate and Cytosolic PH as Modulators of the Synthesis or Consumption of C(4) Organic Acids through NADP-Malic Enzyme in Arabidopsis Thaliana. *Plant Mol Biol* **2013**, *81*, 297–307. https://doi.org/10.1007/s11103-012-9999-6.
52. Badia, M.B.; Arias, C.L.; Tronconi, M.A.; Maurino, V.G.; Andreo, C.S.; Drincovich, M.F.; Wheeler, M.C.G. Enhanced Cytosolic NADP-ME2 Activity in A. Thaliana Affects Plant Development, Stress Tolerance and Specific Diurnal and Nocturnal Cellular Processes. *Plant Sci* **2015**, *240*, 193–203. https://doi.org/10.1016/j.plantsci.2015.09.015.
53. Aghdam, M.S.; Palma, J.M.; Corpas, F.J. NADPH as a Quality Footprinting in Horticultural Crops Marketability. *Trends in Food Science & Technology* **2020**, *103*, 152–161. https://doi.org/10.1016/j.tifs.2020.07.002.
54. Maurino, V.G.; Saigo, M.; Andreo, C.S.; Drincovich, M.F. Non-Photosynthetic "malic Enzyme" from Maize: A Constitutively Expressed Enzyme That Responds to Plant Defence Inducers. *Plant Mol Biol* **2001**, *45*, 409–420. https://doi.org/10.1023/a:1010665910095.
55. Walter, M.H.; Grima-Pettenati, J.; Feuillet, C. Characterization of a Bean (Phaseolus Vulgaris L.) Malic-Enzyme Gene. *Eur J Biochem* **1994**, *224*, 999–1009. https://doi.org/10.1111/j.1432-1033.1994.t01-1-00999.x.
56. Wheeler, M.C.G.; Tronconi, M.A.; Drincovich, M.F.; Andreo, C.S.; Flügge, U.-I.; Maurino, V.G. A Comprehensive Analysis of the NADP-Malic Enzyme Gene Family of Arabidopsis. *Plant Physiol* **2005**, *139*, 39–51. https://doi.org/10.1104/pp.105.065953.
57. Jo, B.-S.; Choi, S.S. Introns: The Functional Benefits of Introns in Genomes. *Genomics Inform* **2015**, *13*, 112–118. https://doi.org/10.5808/GI.2015.13.4.112.
58. Schmitz-Linneweber, C.; Lampe, M.-K.; Sultan, L.D.; Ostersetzer-Biran, O. Organellar Maturases: A Window into the Evolution of the Spliceosome. *Biochim Biophys Acta* **2015**, *1847*, 798–808. https://doi.org/10.1016/j.bbabio.2015.01.009.
59. Fu, Z.-Y.; Zhang, Z.-B.; Hu, X.-J.; Shao, H.-B.; Ping, X. Cloning, Identification, Expression Analysis and Phylogenetic Relevance of Two NADP-Dependent Malic Enzyme Genes from Hexaploid Wheat. *C R Biol* **2009**, *332*, 591–602. https://doi.org/10.1016/j.crvi.2009.03.002.
60. Tao, P.; Guo, W.; Li, B.; Wang, W.; Yue, Z.; Lei, J.; Zhao, Y.; Zhong, X. Genome-Wide Identification, Classification, and Analysis of NADP-ME Family Members from 12 Crucifer Species. *Mol Genet Genomics* **2016**, *291*, 1167–1180. https://doi.org/10.1007/s00438-016-1174-3.
61. Wheeler, M.C.G.; Arias, C.L.; Tronconi, M.A.; Maurino, V.G.; Andreo, C.S.; Drincovitch, M.F. Arabidopsis Thaliana NADP-Malic Enzyme Isoforms: High Degree of Identity but Clearly Distinct Properties. *Plant Mol Biol* **2008**, *67*, 231–242. https://doi.org/10.1007/s11103-008-9313-9.
62. Centeno, D.C.; Osorio, S.; Nunes-Nesi, A.; Bertolo, A.L.F.; Carneiro, R.T.; Araújo, W.L.; Steinhauser, M.-C.; Michalska, J.; Rohrmann, J.; Geigenberger, P.; et al. Malate Plays a Crucial Role in Starch Metabolism, Ripening, and Soluble Solid Content of Tomato Fruit and Affects Postharvest Softening. *Plant Cell* **2011**, *23*, 162–184. https://doi.org/10.1105/tpc.109.072231.
63. Ruffner, H.P.; Possner, D.; Brem, S.; Rast, D.M. The Physiological Role of Malic Enzyme in Grape Ripening. *Planta* **1984**, *160*, 444–448. https://doi.org/10.1007/BF00429761.
64. Carvajal, F.; Palma, F.; Jamilena, M.; Garrido, D. Preconditioning Treatment Induces Chilling Tolerance in Zucchini Fruit Improving Different Physiological Mechanisms against Cold Injury. *Annals of Applied Biology* **2015**, *166*, 340–354. https://doi.org/10.1111/aab.12189.

65. Batista Silva, W.; Cosme Silva, G.M.; Santana, D.B.; Salvador, A.R.; Medeiros, D.B.; Belghith, I.; da Silva, N.M.; Cordeiro, M.H.M.; Misobutsi, G.P. Chitosan Delays Ripening and ROS Production in Guava (Psidium Guajava L.) Fruit. *Food Chem* **2018**, *242*, 232–238. https://doi.org/10.1016/j.foodchem.2017.09.052.
66. Cherian, S.; Figueroa, C.R.; Nair, H. 'Movers and Shakers' in the Regulation of Fruit Ripening: a Cross-Dissection ff Climacteric Versus Non-Climacteric Fruit. *Journal of Experimental Botay* **2014**, *65*, 4705-4722. https://doi.org/10.1093/jxb/eru280.
67. Jarret, R.L.; Berke, T.; Baldwin, E.A.; Antonious, G.F. Variability for Free Sugars and Organic Acids in Capsicum Chinense. *Chem Biodivers* **2009**, *6*, 138–145. https://doi.org/10.1002/cbdv.200800046.
68. de Ï Vila Silva, L.; Condori-Apfata, J.A.; Costa, P.M. de A.; Martino, P.B.O.; Tavares, A.C.A.; Marcelino, M.M.; Raimundi, S.B.C.J.R.; Picoli, E.A. de T.; Araï Jo, W.L.; Zsï Gï N, A.; et al. Source Strength Modulates Fruit Set by Starch Turnover and Export of Both Sucrose and Amino Acids in Pepper. *Plant Cell Physiol* **2019**, *60*, 2319–2330. https://doi.org/10.1093/pcp/pcz128.
69. Selinski, J.; Scheibe, R. Malate Valves: Old Shuttles with New Perspectives. *Plant Biol (Stuttg)* **2019**, *21 Suppl 1*, 21–30. https://doi.org/10.1111/plb.12869.
70. Zhao, Y.; Yu, H.; Zhou, J.-M.; Smith, S.M.; Li, J. Malate Circulation: Linking Chloroplast Metabolism to Mitochondrial ROS. *Trends Plant Sci* **2020**, *25*, 446–454. https://doi.org/10.1016/j.tplants.2020.01.010.
71. Rödiger, A.; Agne, B.; Dobritzsch, D.; Helm, S.; Müller, F.; Pötzsch, N.; Baginsky, S. Chromoplast Differentiation in Bell Pepper (Capsicum Annuum) Fruits. *The Plant Journal* **2021**, *105*, 1431–1442. https://doi.org/10.1111/tpj.15104.
72. González-Gordo, S.; Palma, J.M.; Corpas, F.J. Peroxisomal Proteome Mining of Sweet Pepper (Capsicum Annuum L.) Fruit Ripening Through Whole Isobaric Tags for Relative and Absolute Quantitation Analysis. *Front Plant Sci* **2022**, *13*, 893376. https://doi.org/10.3389/fpls.2022.893376.
73. González-Gordo, S.; Rodríguez-Ruiz, M.; Paradela, A.; Ramos-Fernández, A.; Corpas, F.J.; Palma, J.M. Mitochondrial Protein Expression during Sweet Pepper (Capsicum Annuum L.) Fruit Ripening: ITRAQ-Based Proteomic Analysis and Role of Cytochrome c Oxidase. *J Plant Physiol* **2022**, *274*, 153734. https://doi.org/10.1016/j.jplph.2022.153734.
74. Corpas, F.J.; González-Gordo, S.; Rodríguez-Ruiz, M.; Muñoz-Vargas, M.A.; Palma, J.M. Thiol-Based Oxidative Posttranslational Modifications (OxiPTMs) of Plant Proteins. *Plant Cell Physiol* **2022**, *63*, 889–900. https://doi.org/10.1093/pcp/pcac036.
75. Hu, J.; Huang, X.; Chen, L.; Sun, X.; Lu, C.; Zhang, L.; Wang, Y.; Zuo, J. Site-Specific Nitrosoproteomic Identification of Endogenously S-Nitrosylated Proteins in Arabidopsis. *Plant Physiol* **2015**, *167*, 1731–1746. https://doi.org/10.1104/pp.15.00026.
76. Aroca, A.; Benito, J.M.; Gotor, C.; Romero, L.C. Persulfidation Proteome Reveals the Regulation of Protein Function by Hydrogen Sulfide in Diverse Biological Processes in Arabidopsis. *J Exp Bot* **2017**, *68*, 4915–4927. https://doi.org/10.1093/jxb/erx294.
77. Jones, P.; Binns, D.; Chang, H.-Y.; Fraser, M.; Li, W.; McAnulla, C.; McWilliam, H.; Maslen, J.; Mitchell, A.; Nuka, G.; et al. InterProScan 5: Genome-Scale Protein Function Classification. *Bioinformatics* **2014**, *30*, 1236–1240. https://doi.org/10.1093/bioinformatics/btu031.
78. Thompson, J.D.; Higgins, D.G.; Gibson, T.J. CLUSTAL W: Improving the Sensitivity of Progressive Multiple Sequence Alignment through Sequence Weighting, Position-Specific Gap Penalties and Weight Matrix Choice. *Nucleic Acids Res* **1994**, *22*, 4673–4680.
79. Tamura, K.; Stecher, G.; Kumar, S. MEGA11: Molecular Evolutionary Genetics Analysis Version 11. *Mol Biol Evol* **2021**, *38*, 3022–3027. https://doi.org/10.1093/molbev/msab120.
80. Subramanian, B.; Gao, S.; Lercher, M.J.; Hu, S.; Chen, W.-H. Evolview v3: A Webserver for Visualization, Annotation, and Management of Phylogenetic Trees. *Nucleic Acids Research* **2019**, *47*, W270–W275. https://doi.org/10.1093/nar/gkz357.
81. Bailey, T.L.; Elkan, C. Fitting a Mixture Model by Expectation Maximization to Discover Motifs in Biopolymers. *Proc Int Conf Intell Syst Mol Biol* **1994**, *2*, 28–36.
82. Chen, C.; Chen, H.; Zhang, Y.; Thomas, H.R.; Frank, M.H.; He, Y.; Xia, R. TBtools: An Integrative Toolkit Developed for Interactive Analyses of Big Biological Data. *Mol Plant* **2020**, *13*, 1194–1202. https://doi.org/10.1016/j.molp.2020.06.009.
83. Horton, P.; Park, K.-J.; Obayashi, T.; Fujita, N.; Harada, H.; Adams-Collier, C.J.; Nakai, K. WoLF PSORT: Protein Localization Predictor. *Nucleic Acids Res* **2007**, *35*, W585–W587. https://doi.org/10.1093/nar/gkm259.
84. Sahu, S.S.; Loaiza, C.D.; Kaundal, R. Plant-MSubP: A Computational Framework for the Prediction of Single- and Multi-Target Protein Subcellular Localization Using Integrated Machine-Learning Approaches. *AoB Plants* **2020**, *12*, plz068. https://doi.org/10.1093/aobpla/plz068.
85. Lescot, M.; Déhais, P.; Thijs, G.; Marchal, K.; Moreau, Y.; Van de Peer, Y.; Rouzé, P.; Rombauts, S. PlantCARE, a Database of Plant Cis-Acting Regulatory Elements and a Portal to Tools for in Silico Analysis of Promoter Sequences. *Nucleic Acids Res* **2002**, *30*, 325–327. https://doi.org/10.1093/nar/30.1.325.
86. Langmead, B.; Salzberg, S.L. Fast Gapped-Read Alignment with Bowtie 2. *Nat. Methods* **2012**, *9*, 357–359. https://doi.org/10.1038/nmeth.1923.

 doi:10.20944/preprints202305.1587.v1

87. Li, H.; Handsaker, B.; Wysoker, A.; Fennell, T.; Ruan, J.; Homer, N.; Marth, G.; Abecasis, G.; Durbin, R.; 1000 Genome Project Data Processing Subgroup The Sequence Alignment/Map Format and SAMtools. *Bioinformatics* **2009**, *25*, 2078–2079. https://doi.org/10.1093/bioinformatics/btp352.
88. Gayte, I.G.; Moreno, R.B.; Zonjic, P.S.; Claros, M.G. DEgenes Hunter - A Flexible R Pipeline for Automated RNA-Seq Studies in Organisms without Reference Genome. *Genomics and Computational Biology* **2017**, *3*, 31. https://doi.org/10.18547/gcb.2017.vol3.iss3.e31.